Evidence for Involvement of the Putative First Extracellular Loop in Differential Volume Sensitivity of the Na^+/H^+ Exchangers NHE1 and NHE2[†]

Xiaohua Su, Tianxiang Pang, Shigeo Wakabayashi,* and Munekazu Shigekawa

Department of Molecular Physiology, National Cardiovascular Center Research Institute, Fujishirodai 5-7-1, Suita, Osaka 565-8565, Japan

Received June 20, 2002; Revised Manuscript Received December 2, 2002

ABSTRACT: We studied hyperosmolarity-induced changes in cell volume and cytoplasmic pH in PS120 cells expressing Na^+/H^+ exchanger (NHE) isoforms and their mutants. Change in cell volume was estimated by measuring change in cell height by means of confocal microscopy. Regulatory volume increase (RVI) and cytoplasmic alkalinization were observed in cells expressing NHE1 but not in cells expressing NHE2 or NHE3. Studies using chimeric exchangers revealed that the membrane domain of the exchanger is responsible for the difference in volume sensitivity between NHE1 and NHE2. Although deletion or point mutation within the first extracellular loop of NHE1 did not affect RVI and alkalinization, point mutations within the corresponding region of NHE2, particularly a region containing aa 41−53, as well as replacement of the N-terminus of NHE2 with the corresponding region of NHE1, rendered NHE2 responsive to the activating effect of cell shrinkage. Thus, the membrane domain plays an important role in the response of the exchanger to cell shrinkage. The data suggest that the putative first extracellular loop of NHE2, but not that of NHE1, may exert an inhibitory influence on hyperosmolarity-induced activation of the exchanger and thereby block RVI.

In hyper- or hypoosmotic medium, cell volume rapidly recovers from shrinkage or swelling through processes named regulatory volume increase (RVI)[1] or regulatory volume decrease (RVD) (*1*−*4*). RVI is usually initiated by net uptake of Na^+ and Cl^-, which is accompanied by osmotically obliged water movement. In several cell types, the uptake of NaCl is mediated via functionally coupled Na^+/H^+ exchanger (NHE) and Cl^-/HCO_3^- exchanger (AE) (*1*−*4*). For example, RVI is impaired in the NHE-deficient mutant cell line AP1 derived from Chinese hamster ovary cells (*5*). Similarly, RVI is impaired in *Xenopus* oocytes expressing NHE but lacking anion exchanger (*6*). However, it can be restored when oocytes are transfected with cDNA of the AE2 anion exchanger (*6*).

NHE catalyzes Na^+ influx coupled with H^+ efflux across the plasma membrane. The NHE family comprises eight known isoforms that are thought to differ in tissue localization, inhibitor potency, and mode of regulation, although they have similar overall structures consisting of the N-terminal membrane catalytic domain (∼500 aa) and the C-terminal cytoplasmic regulatory domain (∼300 aa) (*7*−*11*). The molecular mechanisms for regulation of some of these NHE isoforms have been extensively studied. However, the mechanism for cell volume-dependent regulation of NHE isoforms remains largely unknown. The Na^+/H^+ exchanger isoform 1 (NHE1), a ubiquitous isoform, is activated in response to cell shrinkage and thus induces a long-lasting cytoplasmic alkalization (see refs *7* and *11* for reviews). In contrast, the same stress inhibits the activity of NHE3 and thereby induces a large cytoplasmic acidification (*12*, *13*). On the other hand, hyperosmolarity does not induce alkalinization in a NHE-deficient mutant cell line, PS120, expressing NHE2 (*13*, *14*) but does so in a different cell line, AP1, expressing NHE2 (*12*). Therefore, these NHE isoforms appear to respond differently to hyperosmotic stress. In these previous studies of NHE isoforms, a change in cell volume has not been measured.

In this study, we measured hyperosmolarity-induced changes in cell height and intracellular pH in PS120 cells expressing NHE1, NHE2, NHE3, or their mutant variants. A change in cell height was used as an index for a change in cell volume of these adherent cells (see Experimental Procedures and refs *15*−*19*). Hyperosmolarity-induced rapid recovery of cell height as well as cytoplasmic alkalinization was observed only in NHE1-expressing cells. Analysis with chimeric and point mutant exchangers has provided evidence suggesting that the N-terminal portion of the transmembrane domain of the exchanger is responsible for the difference in volume sensitivity between NHE1 and NHE2. In NHE2, the first extracellular loop appears to inhibit hyperosmolarity-induced activation of the exchanger and thus block RVI.

[†] This work was supported by Grant-in-aids on Priority Areas 13142210 and Grant-in-aid 14580664 for Scientific Research from the Ministry of Education, Science, and Culture of Japan and grants from CREST (Core Research for Evolutional Science and Technology) of the Japan Science and Technology Corporation (JST) and the Organization of Pharmaceutical Safety and Research (OPSR) of Japan (Promotion of Fundamental Studies in Health Science). X.S. was supported by the Science and Technology Agency Fellowship of Japan.

* Address correspondence to this author. Phone: 81-6-6833-5012 (ext 2566). Fax: 81-6-6872-7485. E-mail: wak@ri.ncvc.go.jp.

[1] Abbreviations: NHE, Na^+/H^+ exchanger; RVI, regulatory volume increase; pH_i, intracellular pH; EIPA, 5-(*N*-ethyl-*N*-isopropyl)amiloride; HA, hemagglutinin; biotin maleimide, (3-*N*-maleimidylpropionyl)-biocytin; MTSET, 2-(trimethylammonio)ethyl methanethiosulfonate.

10.1021/bi020427d CCC: $25.00
Published on Web 01/03/2003

EXPERIMENTAL PROCEDURES

Materials. Tetramethylrhodamine−dextran and biotin maleimide [3-(*N*-maleimidylpropionyl)biocytin] were purchased from Molecular Probes Inc. MTSET and streptavidin-conjugated agarose were purchased from Toronto Research Chemicals Inc. and Pierce, respectively. The amiloride derivative 5-(*N*-ethyl-*N*-isopropyl)amiloride (EIPA) was a gift from New Drug Research Laboratories of Kanebo, Ltd. (Osaka, Japan). ^{22}NaCl and [7-^{14}C]benzoic acid were purchased from NEN Life Science Products. Rabbit polyclonal antibody (Y-11) against hemagglutinin (HA) epitope was purchased from Santa Cruz Biotechnology, Inc. All other chemicals were of the highest purity available.

Cell Culture and cDNA Transfection. The Na^+/H^+ exchanger deficient cell line PS120 (*20*), provided by Dr. J. Pouysségur (France, Nice), and the corresponding transfectants were maintained in Dulbecco's modified Eagle's medium (Life Technologies, Inc.) containing 25 mM $NaHCO_3$ and supplemented with 7.5% (v/v) fetal calf serum, penicillin (50 units/mL), and streptomycin (50 μg/mL). Cells were maintained at 37 °C in the presence of 5% CO_2. All cDNA constructs were transfected into PS120 cells by the calcium phosphate−DNA coprecipitation technique (*21*), and stable clones were selected by the repetitive H^+-killing selection procedures (*21*).

Construction of NHE Mutant Plasmids. The plasmids carrying cDNAs coding for the Na^+/H^+ exchangers (NHE1 human isoform, NHE2 and NHE3 rat isoforms) were described previously (*14*, *21*). All of the constructs used in this study were produced by a polymerase chain reaction (PCR) based strategy as described (*21*). In this study, we initially introduced a unique restriction site (*Eag*I) corresponding to aa 481 of NHE2 by a PCR-based method. For construction of chimeric exchangers N1N2 and N2N1, DNA fragments corresponding to the C-terminal cytoplasmic domains of NHE1 and NHE2 were produced by PCR using the respective isoform cDNAs as templates and sets of primers containing exogenous restriction sites and incorporated into the *Eag*I/*Xba*I site in NHE2 and the *Acc*I/*Eco*RI site in NHE1 plasmid, respectively. We also employed a similar PCR-based method for construction of other chimeric exchangers between NHE1 and NHE2. For construction of chimeric exchangers of NHE1 whose N-terminal regions were replaced with the corresponding regions of NHE2, we synthesized antisense hybrid primers containing NHE2 regions at the 3′-end and NHE1 regions at the 5′-end. Using these antisense primers and a sense primer annealing to the N-terminus of NHE2, PCR fragments were produced using NHE2 as a template. At the same time, using sense primers complementary to the NHE1 regions of hybrid primers and an antisense primer annealing to NHE1, PCR fragments were produced using NHE1 as a template. These two types of PCR fragments were mixed and subjected to the second PCR reaction. Resultant second PCR products were digested and incorporated into NHE1 cDNA. Chimeric exchangers of NHE2 containing the N-terminal regions of NHE1 were produced in a similar way. Similarly, we produced PCR fragments containing replaced nucleotides for point mutants or nucleotide sequences coding for the influenza virus HA epitope YPYDVPDYAS. These DNA fragments were digested and inserted into appropriate restriction sites in NHE1 and NHE2 plasmids. Inserted DNA fragments were confirmed by sequencing to ensure the fidelity of construction.

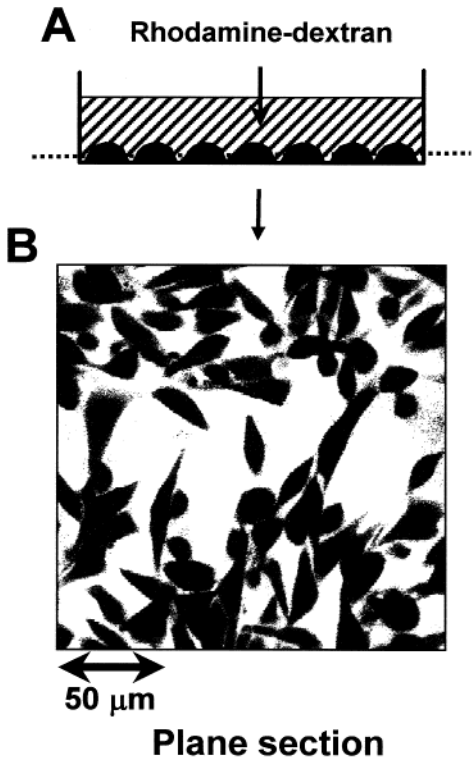

FIGURE 1: Measurement of height of cells attached to a dish. (A) To visualize cell shape, membrane-impermeable tetramethylrhodamine−dextran (0.2 mg/mL) was added to medium. (B) Cells were visualized as nonfluorescent shadows on a confocal fluorescence microscope.

Measurements of Cell Height and Volume. Cells attached to dishes were washed once with 4 mL of serum-free DMEM without phenol red and placed in the same medium containing 0.2 mg/mL membrane-impermeable tetramethylrhodamine−dextran at room temperature to visualize cell shape as a nonfluorescent "shadow" by the fluid labeling method (*22*) (Figure 1). Cells were observed using an MRC-1024 confocal microscope (Bio-Rad) mounted on an Olympus BX50WI fluorescence microscope with a 60× water immersion objective lens. An interface between medium and substratum was determined by taking reflection images (see below). First, we compared hyperosmolarity-induced changes in the height and the volume of the same cells by using the three-dimensional image reconstitution method as described previously (*23*). In these experiments, because image collection took more than 1 min, we used NHE-deficient PS120 cells in which shrinkage was maintained for a relatively long time (see Figure 4A). Before and after induction of shrinkage, 42 optical plane sections (*x*, *y* scan at 512 by 512 pixels) were taken along the *z*-axis at every 0.5 μm (see Figure 1B for an example of one section). Fluorescent images were digitized with 256 intensity levels, and their photometric thresholding was determined empirically with an aid of an imaging software (Scion Image Corp.). Figure 2A,B (lower panels) show contour lines obtained from a cell under control or hyperosmotic conditions. The upper panels represent the vertical sections ($x-z$) constructed along the dotted lines shown in the lower panels. Volume was calculated by multiplying the sum of $x-y$ areas by the *z*-axis distance (0.5 μm). Volume and height of the indicated cell were reduced

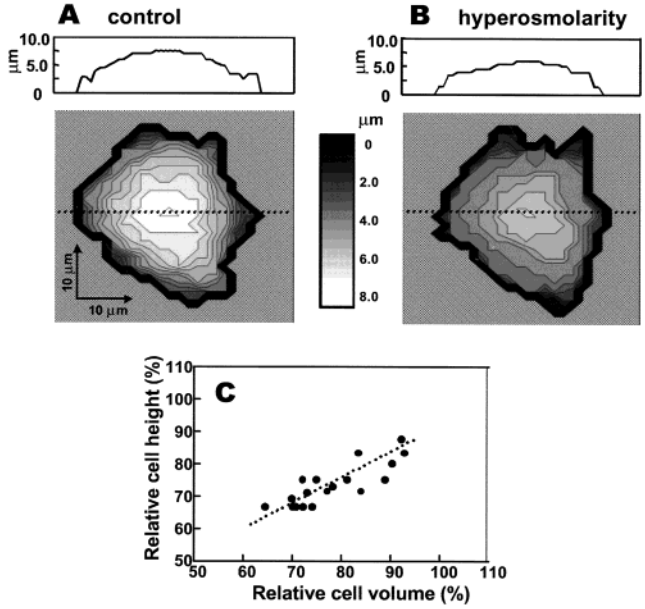

FIGURE 2: Three-dimensional reconstruction from serial optical section images. (A, B) Plane-section images of PS120 cells were taken at 0.5 μm axial intervals under control or hyperosmotic medium (190 mM NaCl) and treated as described under Experimental Procedures. Contour line images were constructed and represented with a gray scale bar. Upper panels show the $x-z$ vertical sections taken along dotted lines shown in lower panels. (C) Relationship between hyperosmotic stress-induced changes in volume and height of 18 cells. Initial values of cell volume and height of individual cells were taken as 100%, and the values of these parameters after shrinkage were normalized to the initial values and plotted in the figure.

from 1.1 to 0.8 pL and 7.5 to 6.0 μm, respectively, upon hyperosmotic stress. Figure 2C shows the relationship between hyperosmolarity-induced changes in volume and height of 18 cells. The initial volume of individual cells varied from 0.7 to 2.0 pL, and the extent of volume change also varied among cells. However, there was significant linear correlation between these two parameters (Figure 2C). Thus, we assume that the change in cell height serves as an index for the change in cell volume at least in our experimental system.

For measurement of time courses of change in cell height, we used 80−90% confluent cells seeded on a 60 mm dish and visualized by fluid labeling as described above. After an $x-y$ plane section image was taken (Figure 1B), a scanning line was chosen in such a way that it passed through near the center of more than five nonoverlapping cells. Vertical cross-section images of cells were reconstructed from scans at that line taken stepwise at every 0.5 μm over a 20 μm focus range (see Figure 3). At the same time, reflection images were taken to visualize an interface between medium and substratum (see dotted lines in Figure 3). Cell edges were determined by an image processing software (Bio-Rad). For each batch of cells expressing individual NHE variants, measurement of cell height change was repeated at least three times, and a representative result is shown in the figure. For each time point, we plotted means ± SD of data from five to seven cells having a cell height above 5 μm (see Figures 3 and 6). Production of a vertical image from line scans usually took about 10 s. We thus used the midpoint of this period for the plot of cell height change. Student's t test was used to evaluate the statistical significance of the difference between cell heights at 30 s and 10 min or later after addition of hyperosmotic medium, and a probability value (P) of less than 0.05 was considered to be significant.

Measurements of pH_i Change and $^{22}Na^+$ Uptake. A change in pH_i was estimated from the distribution of [^{14}C]benzoic acid as described previously (*21*). The stable transfectants grown to confluence in 24-well dishes were serum-depleted for 5 h to maintain the exchanger in the resting state. Cells were further incubated for 1 h at 37 °C in a serum-free, bicarbonate-free DMEM buffered with 20 mM Hepes/Tris (pH 7.0). Cells were then placed for the indicated time in the same medium containing 7 kBq of [^{14}C]benzoic acid/mL with or without 200 mM sucrose. Cells were then rapidly washed four times with ice-cold PBS and solubilized in 0.1 N NaOH, and the ^{14}C radioactivity was counted. Student's t test was used to evaluate the significance of the difference between pH_is before and after addition of hyperosmotic medium, and a probability value (P) of less than 0.05 was considered to be significant.

The $^{22}Na^+$ uptake activity at an acidic pH_i (<6.0) was measured by the NH_4Cl prepulse method as described previously (*21*). Uptake activity was normalized by protein concentration measured by the bicinchoninic assay system (Pierce Chemical Co.) using bovine serum albumin as a standard.

Labeling with Biotin Maleimide. Biotin maleimide labeling of the NHE1 mutant molecules was carried out as described previously (*24*). Briefly, confluent cells were washed twice with PBSCM (phosphate-buffered saline containing 0.1 mM $CaCl_2$ and 1 mM $MgCl_2$) and incubated with or without 5 mM 2-(trimethylammonio)ethyl methanethiosulfonate (MTSET) for 30 min at room temperature. Cells were washed twice with PBSCM and then incubated with 0.5 mM biotin maleimide for 30 min at room temperature. Cells were washed once with PBSCM containing 1% 2-mercaptoethanol and once with PBSCM and collected by centrifugation. Cells were solubilized with lysis buffer containing 1% Triton X-100, 150 mM NaCl, 20 mM Hepes/Tris (pH 7.4), 1 mM PMSF, and 1 mM benzamidine. After centrifugation, the supernatant was mixed with streptavidin−agarose beads, and the mixture was incubated for 1 h at 4 °C with rotation. Agarose beads were washed five times with lysis buffer and then mixed with SDS−PAGE loading buffer containing 3% SDS. Proteins were eluted from beads by boiling for 10 min at 100 °C, separated on an 8.5% acrylamide gel by SDS−PAGE, and subjected to immunoblot analysis with HA antibody. The blots were visualized by the ECL detection system (Amersham Pharmacia Biotech).

RESULTS

Cell Height Change in Transfectants Expressing Wild-Type Exchangers. Figure 3 shows a typical time-dependent change in cell height of NHE1 transfectants upon exposure to hyperosmotic medium containing 190 mM NaCl and 20 mM $NaHCO_3$. As shown in the figure, NaCl at a concentration 50 mM in excess over the physiological level induced fast cell shrinkage, followed by slower recovery. Figure 4 shows summary data for these experiments. In NHE1 transfectants, 190 mM NaCl induced a 20−30% decrease in cell height, followed by a relatively rapid recovery that was completely

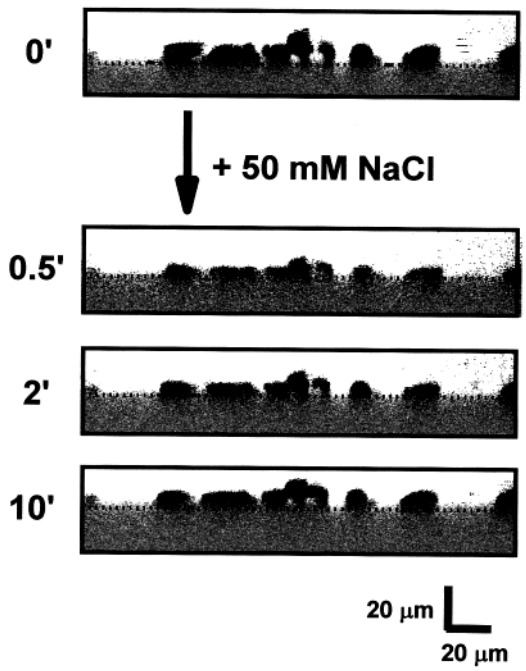

FIGURE 3: Change in cell height induced by hyperosmotic stress. The vertical images of cells expressing NHE1 were observed before and after exposure to high NaCl medium (final NaCl concentration, 190 mM). The experiment was done in serum-free DMEM containing 0.2 mg/mL tetramethylrhodamine−dextran, 20 mM $NaHCO_3$, and 20 mM Hepes/NaOH (pH 7.4). The dotted line in each panel represents the reflection line.

inhibited by the NHE inhibitor EIPA (Figure 4B). We also observed that 100 mM sorbitol or mannitol induced a similar decrease in cell height of NHE1 transfectants, followed by an EIPA-inhibitable recovery [relative cell height, 77.9 ± 5.7% and 97.8 ± 10.6% ($n = 15$, $P < 0.05$) at 1 and 15 min after sorbitol addition and 69.2 ± 12.1% and 93.3 ± 5.7% ($n = 10$, $P < 0.05$) at 1 and 15 min after mannitol addition, respectively]. In this study, we mainly used NaCl instead of sorbitol or mannitol, because the latter was difficult to be mixed rapidly after the addition. The spontaneous recovery in cell height was not observed in exchanger-deficient PS120 cells (Figure 4A), although the height of these cells was rapidly recovered when they were again placed in isoosmotic medium (data not shown). We observed a slower but significant recovery of cell height (more than 90%) in CCL-39 cells with an endogenous NHE1 that exhibited about 10 times less activity compared with NHE1-overexpressing PS120 cells (data not shown). These data suggest that NHE1 is required for volume recovery, consistent with a previous finding that the NHE-deficient mutant cell line AP1 did not exhibit RVI, although the AP1 experiment was done using a different experimental protocol (*5*). In contrast to NHE1 transfectants, NHE2 or NHE3 transfectants did not exhibit a rapid recovery of cell height (Figure 4C,D), although these cells exhibit high Na^+/H^+ exchange activity (see legend to Figure 4). Thus, NHE2 and NHE3 did not confer to PS120 cells the ability to respond to cell volume change.

Cell Height Change in Transfectants Expressing Chimeric or Mutant Exchangers. The results described above show clear differences in the responses of NHEs 1 to 3 to hyperosmotic stress. Because amino acid sequences of NHE1 and NHE2 are fairly homologous to each other (70% amino acid similarity or 53% amino acid identity), we hypothesized that the difference in the osmotic sensitivity arises from the structural difference in the limited regions of these exchangers. We constructed various chimeric exchangers between NHE1 and NHE2 and examined osmotic response in cells expressing them (Figures 5 and 6). In transfectants with two chimeras, E1E2 and E2E1, in which the C-terminal cytoplasmic domains of NHE1 and NHE2 were exchanged with the corresponding domains of NHE2 and NHE1, respectively, recovery of the height was observed in cells expressing E1E2 but not in cells expressing E2E1 (Figure 7A). The result suggests that the N-terminal transmembrane domain is

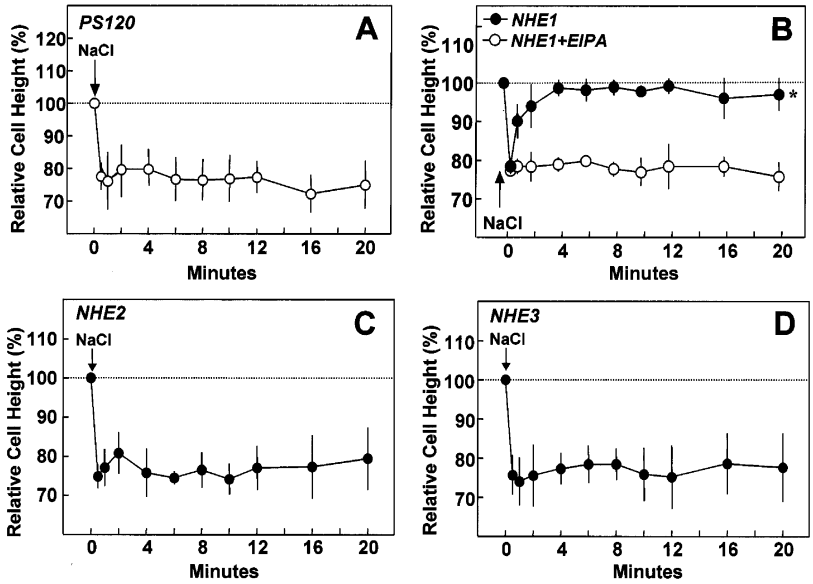

FIGURE 4: Time courses of hyperosmolarity-induced changes in cell height. Changes in cell height were measured in PS120 cells (A) or PS120 cells expressing NHE1 (B), NHE2 (C), or NHE3 (D) placed in serum-free DMEM containing 0.2 mg/mL tetramethylrhodamine−dextran, 20 mM $NaHCO_3$, and 20 mM Hepes/NaOH (pH 7.4). NaCl was added to a final concentration of 190 mM at the time indicated by arrows. In one experiment, medium contained 0.1 mM EIPA (B, open circle). Values are means ± SD of data obtained from five to seven cells (*, $P < 0.05$ versus the cell height at 30 s). EIPA-sensitive $^{22}Na^+$ uptake activity of cells expressing NHE1, NHE2, or NHE3 was 22.4 ± 1.8, 11.1 ± 0.2, or 25.0 ± 0.5 ($n = 3$) nmol mg^{-1} min^{-1}, respectively.

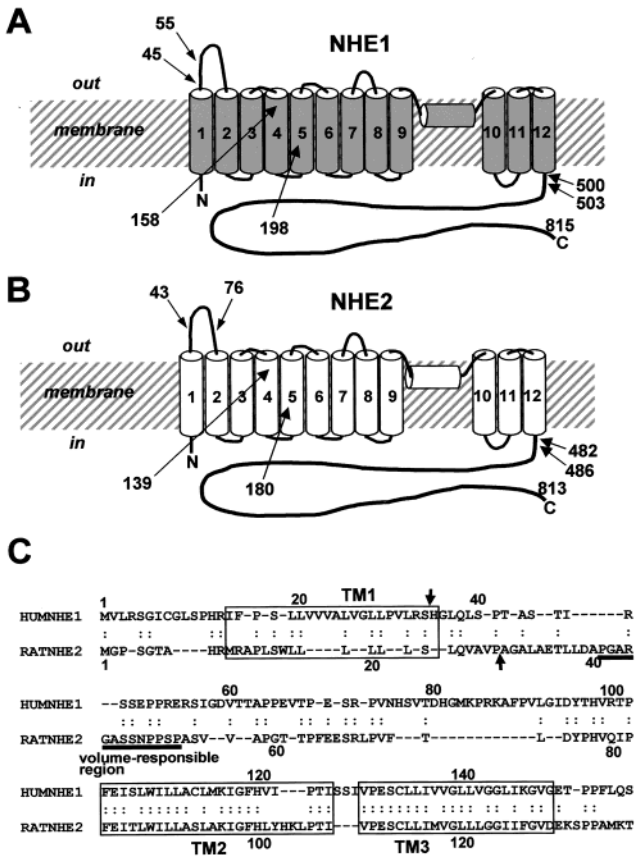

FIGURE 5: Structural models and amino acid sequences of NHE1 and NHE2. (A, B) Topology models for NHE1 and NHE2 deduced from the previous data (*24*). Numbers show approximate positions of amino acid residues corresponding to the junctions between NHE1 and NHE2 in chimeric exchangers. (C) Amino acid sequence alignment between NHE1 and NHE2. TM1−3 show putative transmembrane spanning segments. The identified volume-responsible region of NHE2 is underlined. Arrows indicate the most likely cleavage sites in NHE1 or NHE2 for signal peptidase.

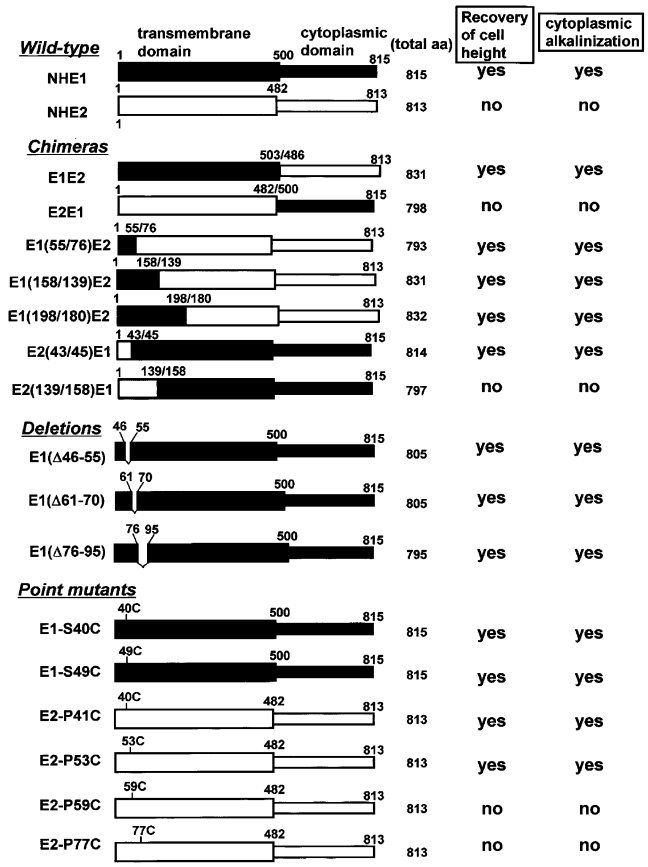

FIGURE 6: Constructs of various NHE variants and their responsiveness to hyperosmotic stress. Chimeric and mutant NHE constructs used in this study are shown. However, some point mutant constructs for NHE2 (P41A, G45C, S48C, P50C, A54C, F72C, and P77A) are not shown (however, see Figure 7). "Yes" on the right indicates the occurrence of significant ($P < 0.05$) recovery of cell height or cytoplasmic alkalinization, while "no" indicates the absence of significant changes in these parameters.

responsible for the differential osmotic responses of these isoforms.

We prepared more than 40 different chimeras involving the transmembrane domains of NHE1 and NHE2. Unfortunately, most of them exhibited no or low exchange activity, which may be due to structural distortion caused by chimera formation. However, recovery of the height was observed in cells expressing E1(55/76)E2 and E2(43/45)E1, in which the N-terminal regions of NHE2 (aa 1−75) and NHE1 (aa 1−44) were replaced by the corresponding regions of NHE1 (aa 1−55) and NHE2 (aa 1−43), respectively (Figure 7B). Recovery of the height of more than 90% was also observed in cells expressing other chimeras, E1(158/140)E2 and E1(198/180)E2 [chimeras are designated as in E1(55/76)E2 and E2(43/45)E1] (data not shown). In contrast, it was not observed in cells expressing E2(139/158)E1, although this mutant exhibited high exchange activity. These results suggest that the N-terminus, in particular, the first extracellular portion of exchanger, is important for the difference in the osmotic responses of NHE1 and NHE2.

We considered two possibilities: (i) the N-terminus of NHE1 functions as a positive regulatory element that renders the chimeric exchangers sensitive to hyperosmotic stress or (ii) the N-terminus of NHE2 functions as a negative regulatory element that renders the chimeric exchangers insensitive. To help to discriminate between these possibilities, we introduced deletion or point mutations into the N-terminus of NHE1 or NHE2. Recovery of the height was observed in cells expressing several deletion mutants, Δ76−95, Δ61−70, and Δ46−55, or point mutants (S40C and S49C) of NHE1 (Figure 7C; data not shown for some mutants). On the other hand, several point mutations in NHE2, i.e., P41C, P50C, and P53C, rendered the exchanger responsive to cell shrinkage, while P59C and P77A did not (Figure 7D; not shown for P50C). Unfortunately, other mutants, such as E1(Δ46−95) and E2(Δ44−75), could not be used in these experiments because of their low expression in cells. The data appear to be consistent with the view that the N-terminus of NHE2 has an inhibitory effect on recovery of cell height.

Hyperosmolarity-Induced Change in Intracellular pH. In the absence of $NaHCO_3$, we observed that hyperosmotic stress such as 200 mM sucrose (Figure 8A) or a concentration of NaCl 100 mM in excess over the physiological level (Figure 8F) induced an EIPA-sensitive cytoplasmic alkalinization in NHE1 transfectants. In contrast, hyperosmotic stress induced cell acidification in NHE2 transfectants (Figure 8A). Since such acidification was also observed in nontransfected PS120 cells, we consider that this acidification is due to intracellular acid production or activation of some H^+-

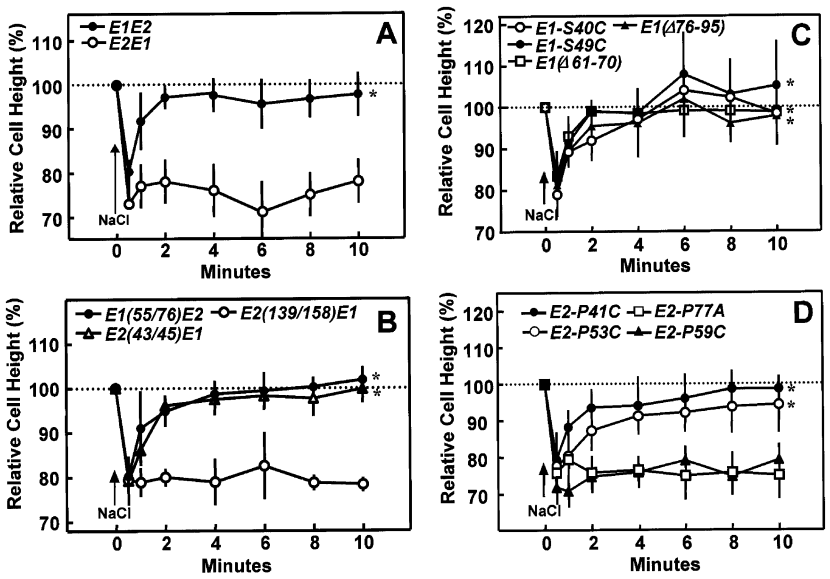

FIGURE 7: Time courses of hyperosmolarity-induced changes in the height of cells expressing various NHE variants. Time courses of cell height change were measured as in Figure 3 in PS120 cells expressing chimeric (A) and deletion or point mutant exchangers for NHE1 (C) or NHE2 (D) after exposing them to 190 mM NaCl at the time indicated by the arrows. EIPA-sensitive $^{22}Na^+$ uptake activities in cells expressing these mutant exchangers ranged between 8 and 27 nmol mg^{-1} min^{-1} (see also Figure 6E for activities of mutant exchangers). Values are means ± SD of data obtained from five to seven cells (*, $P < 0.05$ versus the cell height at 30 s).

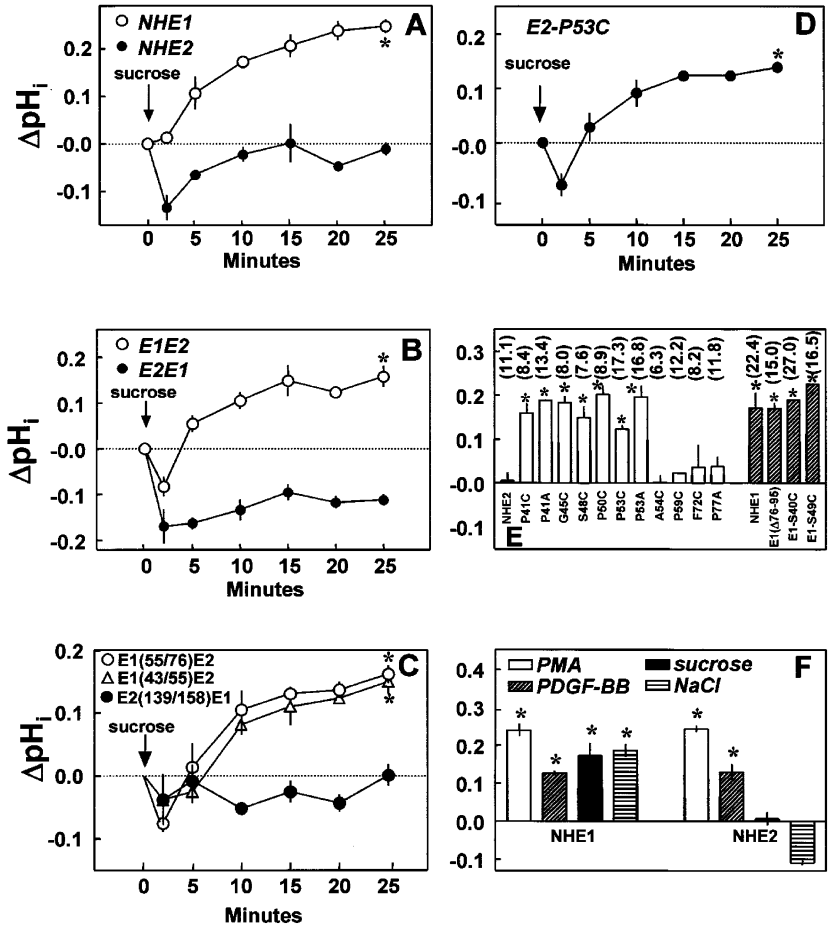

FIGURE 8: Hyperosmolarity-induced cytoplasmic alkalinization in PS120 cells expressing various NHE variants. Time courses of pH_i change were followed in PS120 cells expressing NHE1 or NHE2 (A), E1E2 or E2E1 (B), E1(55/76)E2, E2(43/55)E1, or E2(139/158)E1 (C), or E2-P53C (D) after exposing them to 200 mM sucrose at the time indicated by the arrows. (E) Changes in pH_i in cells expressing NHE2 (open bars) or NHE1 (closed bars) mutants were measured 15 min after the addition of 200 mM sucrose. Values are means ± SD of three determinations. The numbers in parentheses are EIPA-sensitive $^{22}Na^+$ uptake activities (nmol mg^{-1} min^{-1}) of the transfectants carrying respective NHE variants. (F) Effects of various stimuli on pH_i. Cells expressing NHE1 or NHE2 were treated with 1 μM PMA, 100 ng/mL PDGF-BB, 200 mM sucrose, or 240 mM NaCl for 15 min. Values are means ± SD of three determinations (*, $P < 0.05$ versus before stimulation). Resting pH_i before stimulation was in the range of 7.1−7.3 in these experiments.

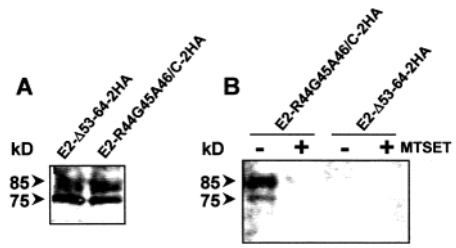

FIGURE 9: Surface labeling of cysteine residues incorporated into the volume-sensitive region of NHE2. Cells expressing HA-tagged NHE2 mutants (E2-Δ54-63-2HA or E2-R44G45A46/C-2HA), which had been treated with or without 5 mM MTSET, were incubated with biotin maleimide, solubilized with the lysis buffer, and then treated with streptavidin−agarose, as described under Experimental Procedures. Total cell lysates (20 μg each) (A) or the proteins recovered with streptavidin−agarose (B) were separated by SDS−PAGE, and exchanger proteins were visualized by immunoblot analysis with HA antibody.

entry pathways caused by cell shrinkage. In NHE2 transfectants, pH_i sometimes recovered to the original level after the initial transient acidification induced by sucrose addition. The latter pH_i recovery was inhibited by EIPA (data not shown). We consider that this recovery was due to activation of NHE2 in response to shrinkage-induced cell acidification, which probably was not sufficient to induce recovery of cell height. In contrast to hyperosmolarity, other stimuli such as PMA and PDGF induced significant cytoplasmic alkalinization in both NHE1 and NHE2 transfectants (Figure 8F), indicating that NHE2 is indeed activated by these stimuli.

We measured the effect of hyperosmolarity on pH_i change in cells expressing various chimeric or point mutant exchangers. Hyperosmolarity induced cytosolic alkalinization in all of the mutant transfectants that exhibited recovery of cell height but not in those showing little such recovery (Figure 8A−E; see also Figure 6). This good correlation between changes in cell height and pH_i supports the view that activation of NHE is required for recovery of cell height. Figure 8E shows the effects of point mutations in the first extracellular portion of the exchanger on the hyperosmolarity-induced cytoplasmic alkalinization in transfectants. Some point mutants of NHE2 (P41C, P41A, G45C, S48C, P50C, P53C, and P53A), but not others (A54A, P59C, F72C, and P77A), induced cytoplasmic alkalinization, suggesting that the region aa 41−53 is important for the response of NHE2 to a change in cell height.

Sidedness of the Volume-Sensitive Region of NHE2. We examined the sidedness of the hyperosmolarity-sensitive region of NHE2 with respect to the membrane by analyzing accessibility of incorporated cysteines to externally applied membrane-impermeable SH reagents. We used cells expressing E2-R44C/G45C/A46C-2HA (Arg44, Gly45, and Ala46 of NHE2 were substituted by cysteines, with the C-terminal end tagged with two HA epitopes). We used cells expressing E2-Δ53-64-2HA (aa 53−64 of NHE2 was deleted) as the control for the cysteine accessibility analysis. Both HA-tagged NHE2 mutants were expressed at similar levels (Figure 9A). For each mutant, we observed two forms of the exchanger with high (85 kDa) or low (75 kDa) molecular mass that are thought to be the O-glycosylated mature or nonglycosylated immature form, respectively (*25*). The cysteine-containing E2-R44C/G45C/A46C-2HA was significantly labeled with externally applied biotin maleimide but not labeled when cells had been pretreated with externally applied membrane-impermeable SH reagent MTSET (Figure 9B). In contrast, E2-Δ53-64-2HA was not labeled with external biotin maleimide even in the absence of MTSET. The data demonstrate that cysteines incorporated into the region of NHE2 involved in volume regulation are exposed on the extracellular side, which is consistent with our previous finding that the corresponding region in NHE1 forms part of the first extracellular loop (*24*).

DISCUSSION

In this study, we measured the hyperosmolarity-induced change in the height of adherent cells expressing various NHE variants by using confocal microscopy and extracellular fluid labeling with a fluorescent dye. Our initial study, in which we compared hyperosmolarity-induced changes in the height and the volume of the same cells measured by the three-dimensional image reconstitution method, suggested that there was significant linear correlation between these two parameters (Figure 2C). We thus assumed that the change in the height of adherent cells serves as a convenient measure of the change in cell volume at least in our experimental system.

The well-documented ion transport systems participating in RVI are the $Na^+/K^+/2Cl^-$ cotransporter and a combination of Na^+/H^+ and Cl^-/HCO_3^- exchangers (*1*−*4*). Coupled activities of the latter exchangers have been shown to be responsible for RVI in many cell types. Our study revealed that cells expressing NHE1 restore their cell height from the hyperosmolarity-induced shrinkage in an EIPA-sensitive manner (see Figures 3 and 4B). Furthermore, in nontransfected PS120 cells lacking NHE activity, a similar recovery of cell height was not observed at least during an initial 20 min after cell shrinkage. Thus, NHE1, presumably with the Cl^-/HCO_3^- exchanger, may play a major role in RVI in our cell system, while the $Na^+/K^+/2Cl^-$ cotransporter contributes minimally.

In contrast to cells expressing NHE1, cells expressing NHE2 or NHE3 did not recover their cell height rapidly after shrinkage (see Figure 4), suggesting that they are not responsive to a change in cell volume. Consistent with this finding, hyperosmolarity induced cytoplasmic alkalinization in cells expressing NHE1 but not in cells expressing NHE2 or NHE3 (Figure 8; see also refs *13* and *14*). The data suggest that these NHE isoforms may possess regions conferring different volume sensitivity. We used a chimera strategy involving NHE1 and NHE2 to search for such regions. Cells expressing a chimeric exchanger, E1E2, showed recovery of cell height and cytoplasmic alkalinization, while a reciprocal chimeric exchanger, E2E1, did not (Figure 7A). Thus, the transmembrane domain of the exchanger is important for the shrinkage-induced activation of the exchanger. This result appears to be consistent with a previous finding that an NHE1 mutant (Δ566) having a large deletion of the C-terminal cytoplasmic domain is activated in response to hyperosmotic stress (*26*).

Recovery of cell height and cytoplasmic alkalinization were observed in cells expressing several other chimeric exchangers, E1(55/76)E2, E1(158/139)E2, and E1(198/180)E2, in which the N-terminus of NHE2 was replaced by the corresponding regions of NHE1 but not in cells express-

ing a reciprocal chimeric exchanger, E2(139/158)E1 (see Figures 7B and 8C and Results). These data suggest that the N-termini of exchangers are important for the differential responses of NHE1 and NHE2. The result shown in Figure 9 suggests that the region (aa 25−85) of NHE2 corresponding to aa 35−110 of NHE1 is exposed on the external side. We do not know whether the N-terminus of NHE2 is cleaved off or not as the signal peptide. If it is not cleaved off, the NHE2 region (aa 25−85) is mapped to the first extracellular loop (see below). Interestingly, amino acid sequences of the N-termini of NHE1 and NHE2 are very different (see Figure 5C), despite the fact that the remaining portions of the transmembrane domain of both isoforms are highly homologous (~70% amino acid identity). Such divergence in the sequence may provide a structural basis for the observed functional difference between the two isoforms.

Recovery of cell height and cytoplasmic alkalinization were observed in cells expressing several deletion or point mutants in the first extracellular loop of NHE1, Δ76−95, Δ61−70, Δ46−55, S40C, and S49C (see Figures 7C and 8E). In addition, these two events were observed in a chimeric exchanger, E2(43/55)E1, in which the N-terminal 44 amino acids of NHE1 were replaced by the corresponding 43 amino acids of NHE2 (see Figures 7B and 8C). These data suggest that the N-terminal region (aa 1−95) of NHE1 encompassing the cytosolic N-tail, the first transmembrane segment, and the first extracellular loop is not involved in the volume-sensing mechanism of NHE1.

In NHE2, not as in NHE1, mutations in the first extracellular loop caused a remarkable change in the volume-dependent regulation of exchange activity; surprisingly, some mutations at single residues introduced into the N-terminus (aa 41−53) rendered the exchanger activatable by cell shrinkage, although other mutations did not (Figures 7B and 8E). Furthermore, a chimeric exchanger, E2(139/158)E1, was not activated by cell shrinkage, although E2(43/55)E1 showed recovery of cell height and alkalinization as noted above. Together, these results suggest that the first extracellular loop of NHE2 exerts an inhibitory influence on shrinkage-induced activation of the exchanger and thus blocks RVI. Such an inhibitory action of the first extracellular loop of NHE2 and the absence of regulatory influence of the corresponding segment of NHE1 may explain why several NHE2 chimeras carrying the N-terminal NHE1 segments, i.e., E1(55/76)E2, E1(158/139)E2, and E1(198/180)E2, are activated by cell shrinkage.

According to an algorithm for prediction of signal sequence, the NHE isoforms NHE1−7 were predicted to contain signal peptides.[2] Indeed, it has been reported on the basis of in vitro translation experiments that the N-termini of NHE3 (*27*) and NHE1 (*28*) are cleaved off as signal peptides. However, we previously found that Cys-8 in the N-tail of NHE1 was labeled with biotin maleimide only after cells were permeabilized, suggesting that the N-tail of NHE1 is retained in the cytosol at least partly (*24*). Therefore, we are not certain about the extent to which the mature NHE1 expressed in the plasma membrane retains the N-tail in the cytosol. Further experiments such as determination of the N-terminal amino acid sequences of mature NHE isoforms would be required to obtain an unambiguous conclusion. It should be noted, however, that the predicted cleavage sites in NHE1 and NHE2 are located in regions N-terminal to the functionally important regions identified in this study (see Figure 5C).

We previously showed that surface biotinylation of substituted cysteine residues in the first extracellular loop of NHE1 was not uniform (*24*), suggesting that the loop is not completely exposed externally and may form a compact folded structure. This loop may not functionally interact with other important region(s) of the exchanger, because deletions within it did not significantly influence the shrinkage-induced activation of NHE1 (see above). In contrast, the first extracellular loop of NHE2 appears to functionally interact with other region(s) of the exchanger, because this region of NHE2 is highly mutation-sensitive and such mutations render the exchanger sensitive to cell shrinkage (see above). The first extracellular loop of NHE2 could interact with other region(s) of the transmembrane domain of the exchanger or other adjacent proteins. In this context, it is interesting to note that, in the cystic fibrosis transmembrane conductance regulator, disease-associated point mutations in extracellular loops 1, 2, and 4 exert a significant influence on the stability of the channel pore (*29*).

We currently have little information regarding how NHE1 and NHE2 with mutations in the first extracellular loop are activated in response to cell shrinkage. It is possible that the exchanger directly senses a change in membrane strain imposed by cell shrinkage. One example of membrane proteins that directly sense membrane strain is the bacterial stretch-activated channel MscL (*30*, *31*). Furthermore, two recent studies have shown that an osmoregulated ABC transporter OpuA of *Lactococcus latis* (*32*) and a betanine carrier BetP of *Corynebacterium glutamicum* (*33*) are activated in response to hyperosmotic stress when purified proteins were reconstituted in proteoliposomes that are devoid of all other cellular proteins, strongly suggesting that transporter activation by a transmembrane osmotic gradient is mediated via changes in membrane properties such as membrane strain, curvature stress, or protein−lipid interactions. On the other hand, previous literature also reported that cell shrinkage-induced activation of NHE1 occurs via intracellular events involving several families of protein kinases (*34*−*37*) or a Cl^--dependent, G-protein-mediated process (*38*) or Ca^{2+}/calmodulin-dependent process (*39*). It is not clear how these intracellular events are related to the membrane events that we have seen in this study.

In summary, we presented evidence that the first extracellular loop is responsible for the differential volume sensitivity of NHE1 and NHE2. The data suggest that the first extracellular loop of NHE2, but not that of NHE1, may exert an inhibitory influence on hyperosmolarity-induced activation of the exchanger. Thus, the exchanger may not be activated simply through intracellular signaling events caused by cell shrinkage. Our present findings provide new information regarding cell shrinkage-induced activation of the Na^+/H^+ exchanger.

REFERENCES

1. Demaurex, N., and Grinstein, S. (1994) *J. Exp. Biol. 196*, 389−404.
2. Grinstein, S., and Foskett, J. K. (1990) *52*, 399−414.

[2] Prediction was made on the World Wide Web.

3. Haussinger, D. (1996) *Biochem. J. 313*, 697−710.
4. Lang, F., Busch, G. L., Ritter, M., Volkl, H., Wakdegger, S., Gulbins, E., and Haussinger, D. (1998) *Physiol. Rev. 78*, 247−306.
5. Rotin, D., and Grinstein, S. (1989) *Am. J. Physiol. 257*, C1158−C1165.
6. Jiang, L., Chernova, M. N., and Alper, S. L. (1997) *Am. J. Physiol 272*, C191−C202.
7. Orlowski, J., and Grinstein, S. (1997) *J. Biol. Chem. 272*, 22373−22376.
8. Orlowski, J., Kandasamy, R. A., and Shull, G. E. (1992) *J. Biol. Chem. 267*, 9331−9339.
9. Sardet, C., Franchi, A., and Pouysségur, J. (1989) *Cell 56*, 271−280.
10. Tsé, C. M., Levine, S. A., Yun, C. H. C., Montrose, M. H., Little, P. J., Pouysségur, J., and Donowitz, M. (1993) *J. Biol. Chem. 268*, 11917−11924.
11. Wakabayashi, S., Shigekawa, M., and Pouysségur, J. (1997) *Physiol. Rev. 77*, 51−74.
12. Kapus, A., Grinstein, S., Wasan, S., Kandasamy, R., and Orlowski, J. (1994) *J. Biol. Chem. 269*, 23544−23552.
13. Nath, S. K., Hang, C. Y., Levine, S. A., Yun, C. H. C., Montrose, M. H., Donowitz, M., and Tsé, C. M. (1996) *Am. J. Physiol. 270*, G431−G441.
14. Kobayashi, Y., Pang, T., Iwamoto, T., Wakabayashi, S., and Shigekawa, M. (2000) *Pfluegers Arch. 439*, 455−462.
15. Roy, G., and Sauvé, R. (1987) *J. Membr. Biol. 100*, 83−96.
16. Crowe, W. E., and Wills, N. K. (1991) *Pfluegers Arch. 419*, 349−357.
17. van Driessche, W., Smet, P. D., and Raskin, G. (1993) *Pfluegers Arch. 425*, 164−171.
18. Wong, C.-S., Lui, P.-Y., and Kong, S.-K. (1999) *Bioimages 7*, 113−120.
19. Wang, Z., Mitsuiye, T., Rees, S. A., and Noma, A. (1997) *J. Gen. Physiol. 110*, 73−82.
20. Pouysségur, J., Sardet, C., Franchi, A., L'Allemain, G., and Paris, S. (1984) *Proc. Natl. Acad. Sci. U.S.A. 81*, 4833−4837.
21. Wakabayashi, S., Fafournoux, P., Sardet, C., and Pouysségur, J. (1992) *Proc. Natl. Acad. Sci. U.S.A. 89*, 2424−2428.
22. Murakami, T., Ono, M., and Ishikawa, H. (1993) *Bioimages 1*, 1−8.
23. Sato, H., Delbridge, L. M. D., Blatter, L. A., and Bers, D. M. (1996) *Biophys. J. 70*, 1494−1504.
24. Wakabayashi, S., Pang, T., Su, X., and Shigekawa, M. (2000) *J. Biol. Chem. 275*, 7942−7949.
25. Tsé, C. M, Levine, S. A., Yun, C. H. C., Khurana, S., and Donowitz, M. (1994) *Biochemistry 33*, 12954−12961.
26. Bianchini, L., Kapus, A., Lukacs, G., Wasan, S., Wakabayashi, S., Pouysségur, J., Yu, F. H., Orlowski, J., and Grinstein, S. (1995) *Am. J. Physiol. 269*, C998−C1007.
27. Zizak, M., Cavet, M. E., Bayle, D., Tsé, C.-M., Hallen, S., Sachs, G., and Donowitz, M. (2000) *Biochemistry 39*, 8102−8112.
28. Miyazaki, E., Sakaguchi, M., Wakabayashi, S., Shigekawa, M., and Mihara, K. (2001) *J. Biol. Chem. 276*, 49221−49227.
29. Hämmerle, M. M., Aleksandrov, A. A., and Riordan, J. R. (2001) *J. Biol. Chem. 276*, 14848−14854.
30. Sukharev, S. I., Blount, P., Martinac, B., and Kung, C. (1997) *Annu. Rev. Physiol. 59*, 633−657.
31. Wood, J. M. (1999) *Microbiol. Mol. Biol. Rev. 63*, 230−262.
32. van der Heide, T., and Poolman, B. (2000) *Proc. Natl. Acad. Sci. U.S.A. 97*, 7102−7106.
33. Rübenhagen, R., Rönsch, H., Jung, H., and Krämer, R. (2000) *J. Biol. Chem. 275*, 735−741.
34. Wesselborg, S., Bauer, M. K. A., Vogt, M., Schmitz, M. L., and Schulze-Osthoff, K. (1997) *J. Biol. Chem. 272*, 12422−12429.
35. Gatsios, P., Terstegen, L., Schliess, F., Haussinger, D., Kerr, I. M., Heinrich, P. C., and Graeve, L. (1998) *J. Biol. Chem. 273*, 22962−22968.
36. Kapus, A., Szaszi, K., Sun, J., Rizoli, S., and Rotstein, O. D. (1999) *J. Biol. Chem. 274*, 8093−8102.
37. Shrode, L. D., Klein, J. D., O'Neill, C., and Putnum, R. W. (1995) *Am. J. Physiol. 269*, C257−C266.
38. Hogan, E. M., Davis, B. A., and Boron, W. F. (1997) *J. Gen. Physiol. 110*, 629−639.
39. Bertrand, B., Wakabayashi, S., Ikeda, T., Pouysségur, J., and Shigekawa, M. (1994) *J. Biol. Chem. 269*, 13703−13709.

BI020427D